Accepted Manuscript

Title: Over-expression of the *CHS* gene enhances resistance of *Arabidopsis* leaves to high light

Authors: Xiao-Hong Zhang, Xiao-Ting Zheng, Bei-Yu Sun, Chang-Lian Peng, Wah Soon Chow

PII: S0098-8472(17)30331-3
DOI: https://doi.org/10.1016/j.envexpbot.2017.12.011
Reference: EEB 3351

To appear in: *Environmental and Experimental Botany*

Received date: 23-10-2017
Revised date: 7-12-2017
Accepted date: 9-12-2017

Please cite this article as: Zhang, Xiao-Hong, Zheng, Xiao-Ting, Sun, Bei-Yu, Peng, Chang-Lian, Chow, Wah Soon, Over-expression of the CHS gene enhances resistance of Arabidopsis leaves to high light.Environmental and Experimental Botany https://doi.org/10.1016/j.envexpbot.2017.12.011

Over-expression of the *CHS* gene enhances resistance of *Arabidopsis* leaves to high light

Xiao-Hong Zhang[a,1], Xiao-Ting Zheng[a,1], Bei-Yu Sun[a], Chang-Lian Peng[a,*], Wah Soon Chow[b,*]

[a] Guangdong Provincial Key Laboratory of Biotechnology for Plant Development, Guangzhou Key Laboratory of Subtropical Biodiversity and Biomonitoring, School of Life Sciences, South China Normal University, Guangzhou 510631, PR China

[b] Division of Plant Sciences, Research School of Biology, College of Science, The Australian National University, Acton, Australian Capital Territory 2601, Australia

* Corresponding author.

E-mail addresses: pengchl@scib.ac.cn (C.-L. Peng), Fred.Chow@anu.edu.au (W.S. Chow).

[1] Co-first authors: These authors contributed equally to this work.

Highlights

- We constructed *CHS*-overexpression *Arabidopsis thaliana* lines, and selected them as well as the anthocyanin-deficient mutant (*tt4*), and *Arabidopsis* ecotype Columbia (*Col*) for experiments.
- *CHS*-overexpression *Arabidopsis thaliana* lines enhances HL resistance by synthesizing more anthocyanins.
- Anthocyanin enhance the adaptability of plants to high light and maintain photosynthetic capacity via both antioxidation and attenuation of light.

ABSTRACT

Previous studies have suggested that high light (HL) stress causes photoinhibition in plants, while anthocyanins could protect the photosynthetic apparatus against photoinhibition. However, the photoprotection mechanism of anthocyanins is still ambiguous. We studied physiological

responses and molecular changes for *CHS*-overexpression lines (*CHS1*, *CHS2*, *CHS3*), *Arabidopsis thaliana* ecotype Columbia (*Col*), and T-DNA insertion lines of *CHS* (*tt4*) under HL (200 μmol m^{-2} s^{-1}) to explore the photoprotection mechanism of anthocyanins. The results showed that HL induced anthocyanin synthesis and accumulation. The leaves of *CHS*-overexpression lines turned reddest and the genes, including CHS, DFR, ANS, were expressed at highest levels. Thus, the *CHS*-overexpression lines maintained the highest photosynthetic capacity and suffered the least damage from HL of the three phenotypes. However, the CHS enzyme and anthocyanins were undetectable in *tt4* during the experiment. Correspondingly, chlorophyll fluorescence parameters of *tt4* declined greatly. The photosynthetic apparatus and cell membranes were also impaired dramatically. The physiological characteristics of *Col* were compared between *CHS*-overexpression lines and *tt4*. Together, the results suggest that over-expression of *CHS* gene enhances HL resistance by synthesizing more anthocyanins, that anthocyanins enhance the adaptability of plants to HL and that they maintain photosynthetic capacity via both antioxidation and attenuation of light.

***Key words**:* CHS; high light; anthocyanins; photoprotection; antioxidation

1. Introduction

Anthocyanins are a group of polyphenol flavonoids that provide plant organs with a wide range of colors ranging from orange/red to violet/blue. Over 600 anthocyanins have been isolated from various plants species (Andersen and Jordheim 2005). Anthocyanins are the products from a branch path of flavonoid metabolism (Grotewold 2006). At the beginning of anthocyanin synthesis, chalcone synthase (CHS) catalyzes the synthesis of naringenin chalcone from three molecules of 4-malonyl-CoA, and one molecule of *p*-coumaroyl CoA. CHS is the first key enzyme in the biosynthesis of flavonoids (Tanaka at al., 2008).

The process of anthocyanin synthesis in plants is regulated by many environmental and growth factors, such as illumination (Oren-Shamir 2009), fungi (Gläßgen et al., 1998), sucrose level (Teng et al., 2005), salt concentration (Oh et al., 2011), temperature (Catalá et al., 2011) and nutrition level (Rubin et al., 2009). Illumination includes illumination intensity and light quality.

Photoperiod is one of the most important environmental factors (Howe et al., 1995). Previous studies have shown that the absorption spectra of anthocyanins overlap with those of photosynthetic pigments, roughly ranging from 400 nm to 600 nm (Karageorgou and Manetas 2006). For the optical masking of green light, anthocyanins have very sharp peaks in absorbance centered around 520-530 nm and low absorption at the blue and red wavelengths (Neill and Gould, 2003). Red light and blue light are the main lights used in photosynthesis (Gould at al., 2002). Anthocyanins and photosynthetic pigments are all affected by illumination intensity, suggesting a potential relationship between light absorption by anthocyanins and photosynthetic pigments. In addition, anthocyanins affect the photosynthetic capacity of plants (Olaizola and Duerr 1990; Oren-Shamir 2009). In the natural environment, high light (HL, ≈2000 μmol m^{-2} s^{-1}), high temperature and other environmental stresses often occur simultaneously. Then plant growth can be limited due to photoinhibition, which is the decline in the quantum yield of photosynthesis caused by excess light. Photoinhibition can be quantitatively analyzed by PAM chlorophyll fluorometry (Genty et al., 1989; Krause and Weis, 1998).

Many plants have red leaves in nature. The ability to absorb green and blue light is greater in leaves that are rich in anthocyanins than those without anthocyanins (Neill and Gould, 2003; Merzlyak et al., 2008). Anthocyanins can attenuate the light reaching the chloroplast, thereby alleviating photoinhibition to protect the photosynthetic apparatus (Steyn et al., 2002; Gould at al., 2002). It has been pointed out that photoprotection facilitated by anthocyanins is vital to plants which are under various stresses. Previous studies suggested that *Arabidopsis thaliana* wild type (WT) was more resistant than deficient mutants *tt3* and *tt4* to different stresses, implying that flavonoids, especially anthocyanins, further protect the photosynthetic apparatus under severe stresses (Shao et al., 2007; Zhang et al., 2012). Similarly, seedlings of *Ocimum gratissimum* suffered severe chilling injury in HL (1000 μmol m^{-2} s^{-1}) intensity under the pretreatment of low-temperature, whereas seedlings of *O. basilicum* 'purple ruffles' rich in anthocyanins showed normal or near normal function (Tian et al., 2013). HL induces the accumulation of anthocyanins in young leaves of *Schima superba* (Zhang et al., 2017). Zeng et al. (2010) found that when supplemental anthocyanins were infiltrated into leaves of the anthocyanin-deficient double mutant (*tt3tt4*), exogenous anthocyanins alleviated direct or indirect oxidative damage of the

photosynthetic apparatus and DNA in plants under HL stress.

Reactive oxygen species (ROS) are important signaling molecules, but excess ROS damage the cell membranes, phospholipids, proteins and nucleic acids. They increase the permeability of cell membrane and the peroxidation of membrane lipids, thereby damaging the structure and function of plant cells (Donahue et al., 1997; Xu et al., 2017). Antioxidative systems have evolved to scavenge ROS and improve the resistance of plants through a long evolutionary progress. Antioxidative enzymes, such as superoxide dismutase (SOD), catalase (CAT), ascorbate peroxidase (APX) and glutathione reductase (GR), are major players that detoxify ROS (Mittler 2002). Furthermore, many low molecular weight antioxidants (LMWA), like ascorbic acid (vitamin C), tocopherol (Vitamin E), glutathione (GSH), β-carotene, phenolic compounds and flavonoids, also play an important role in antioxidation. It has been demonstrated that the antioxidative capacity of flavonoids is about four-fold greater than vitamin C and vitamin E (Rice-Evans et al., 1997; Lee and Gould, 2002). As a sub-group of flavonoids, anthocyanins play an important role in photoprotection. For one thing, anthocyanins can decrease the degree of ROS accumulation by absorbing and blocking out part of excess blue-violet light to protect mesophyll cells underneath the epidermis. For another, anthocyanins can eliminate ROS to ease the damage due to photooxidation. Previous studies have confirmed that *Galax urceolata*, a tufted evergreen perennial herb, could accumulate more anthocyanins in leaves under HL during winter. The colour of leaves changed from green to red in winter, presenting strong evidence for light attenuation and antioxidative activity of anthocyanins (Hughes and Smith, 2007). *Zea mays* could accumulate anthocyanins in leaves to protect chloroplasts and prevent photoinhibition at low temperature, thereby improving photosynthetic efficiency (Pietrini et al., 2002). Those researchers all suggested that anthocyanins ameliorated photodamage under stress, especially under HL stress.

At present, much of the research on abiotic stress focuses on the HL response mechanisms of different plants, such as *Arabidopsis thaliana* (Barczak-Brzyżek et al. 2017; Schumann et al. 2017; Zeng et al. 2017); *Begonia semperflorens* (Wang et al. 2017); *Solanum lycopersicum L.* (Lu et al. 2017); *Cucumis sativus* (Chen et al. 2017; Yu et al., 2016); *Oryza sativa L.* (Faseela and Puthur 2016); and *Acer saccharum Marsh.* (Singh et al. 2016). What can be considered HL intensity varies from plant to plant, depending on the biotope and light saturation point (LSP) of species

(Demmig-Adams and Adams Iii, 1992; Schumann et al. 2017). However, the mechanism by which anthocyanins protect the chloroplast and prevent HL stress is still not very clear, necessitating further research to obtain more evidence to support it.

In this study, we investigated the effects of anthocyanins on *Arabidopsis thaliana* ecotype Columbia (*Col*), *CHS*-overexpression lines (*CHS1*, *CHS2*, *CHS3*) and T-DNA insertion lines of *CHS* (*tt4*) under HL (200 μmol m^{-2} s^{-1}, which is twice as high as the normal growth light intensity). We analyzed expression levels of anthocyanin biosynthesis related genes, and physiological responses of *Arabidopsis thaliana*. We hypothesized that (1) *CHS*-overexpression lines have greater resistance to HL treatment and over-expression of the *CHS* gene enhances HL resistance by synthesizing more anthocyanins, and (2) anthocyanins enhance the ability of a plant to acclimate to HL via both antioxidation and attenuation of light.

2. Materials and methods

2.1 Plant materials and growth conditions

Seeds of *Arabidopsis thaliana* ecotype Columbia (*Col*) and T-DNA insertion mutant at *CHS*, *tt4* (SALK_020583) were obtained from the Arabidopsis Biological Resource Center (ABRC), the Ohio State University, Columbus, OH, USA. The seed coat of the *Col* is brown, while the coat of the mutant is yellow. Seeds were imbibed at 4°C in the dark for 3 days to synchronize germination, and then sown on sterilized MS medium for approximately 10 d. Plant seedlings were transferred to soil (peat soil:vermiculite = 3:1) in a growth cabinet, the conditions of which were 20-22°C with a 16-h photoperiod (photosynthetic photon flux density, PPFD = 100 μmol m^{-2} s^{-1}) and a relative humidity of 80%.

2.2 Construction of the CHS-overexpression transgenic lines

Arabidopsis thaliana ecotype Columbia (*Col*) was used for constructing *CHS*-overexpression transgenic lines in this experiment. A full-length *CHS* (TAIR ID: AT5G13930) cDNA was cloned by RT-PCR using the following primer pair: 5'-TAGGTACCCATGGTGATGGCTGGTGCTTC-3' and 5'-TAGGATCCTTAGAGAGGAACGCTGTGCAAG-3' (Table 1). The cDNA was introduced into a pMD18-T vector (Takara Co., Japan) and verified by sequencing. The plasmid DNA

harboring the full-length fragment of *CHS* was digested with *Kpn*I and *BamH*I, and then subcloned into the corresponding sites of the binary vector *pCanGmyc* under the control of CaMV 35S promoter. The constructed plasmid was transferred into *Arabidopsis thaliana* ecotype Columbia via the Agrobacterium-mediated floral dipping transformation method (Clough and Bent1998). Homozygous transgenic progeny lines were obtained through the kanamycin-resistance test and quantitative RT-PCR analysis.

2.3 RNA extraction and cDNA synthesis

Total RNA was extracted with TRIzol regent (Invitrogen) from mature rosette leaves according to a standard TRIzol (Invitrogen) protocol. The RAN was treated with DNase I (Takara) prior to synthesis the first strand of cDNA with oligo (dT) 18 primer and the M-MLV reverse transcriptase kit (Takara).

2.4 qRT-PCR of CHS, DFR and ANS genes

Gene specific qRT-PCR primers were designed using Premier 5.0 software (Premier Biosoft International, Palo Alto, CA). The specific primer pairs are shown in Table 2. qRT-PCR for gene expression involved in the anthocyanin pathway (*CHS*, *DFR*, *ANS*), was performed using an Applied Biosystem platform. Each 10 μL of reaction solution contained: 5.2μL SYBR® *Premix* EX Tap™ II (Takara), 0.4 μL of each primer, 0.5 μL cDNA, 3.5 μL DEPC water. The reaction cycle was 95°C for 30s, followed by 40 cycles (95°C for 5s, 60°C for 34s), and 1 cycle for recording a melt curve at 95°C for 15 s and 60°C for 1 min. The relative expression levels of *CHS*, *DFR* and *ANS* in the leaves were quantified relative to the *TUB* gene and calculated using the $2^{-\Delta\Delta Ct}$ method (Livak and Schmittren, 2001).

2.5 High light treatments.

Seedlings were grown on soil (peat soil: vermiculite = 3:1) in a growth chamber under normal conditions at a light intensity of 100 μmol photons m^{-2} s^{-1} for 25 days. The plants were

then subjected high light treatment at 200 μmol photons m^{-2} s^{-1}.

2.6 Quantification of pigments

Anthocyanins were measured using the methods described by Wade et al. (2003) with some modification. Fresh leaf material (0.05 g) was extracted in 3 ml of 1% HCl in methanol (v/v), and the extracts were kept in dark at 4°C overnight. Subsequently, chloroform and deionized water were added to the extract for removal of chlorophylls. After blending and settling, anthocyanins were dissolved in the upper water phase. The supernatant absorption spectra were recorded from 400 to 700 nm. Spectrophotometric analysis of the methanol extracts was conducted with a Visible-UV spectrophotometer (Lambda25, Perkin-Elmer, Waltham, MA, USA).

2.7 Chlorophyll fluorescence measurements

Chlorophyll fluorescence was measured using a portable pulse-modulated fluorometer (PAM 2100, Walz, Effeltrich, Germany). The leaves were dark-adapted for 20 min prior to PAM fluorescence determination. The initial fluorescence (Fo) was determined with a weak modulated light (0.04 μmol m^{-2} s^{-1}). The maximal fluorescence (Fm) was induced by a saturating pulse of light (6000 μmol m^{-2} s^{-1}) applied over 0.8 s. Fm' was monitored with a saturating pulse following 15 min of continuous actinic light (200 μmol m^{-2} s^{-1}). The primary photochemical efficiency of photosystem II (PSII) (Fv/Fm), the ETR through PSII, the photochemical quenching coefficient (qP), and yield were calculated according to Gray et al. (2003) and Schreiber et al. (1986).

2.8 Determination of Rubisco protein

Rubisco protein determination was carried out by following the procedures described by Zhang et al. (2016) and Rubisco large subunit (RL) was further identified using immunoblotting analysis.

2.9 H_2O_2 and $^{\bullet}O_2^-$ localization in situ

ROS localization was conducted according to Romero-Puertas et al. (2004) and Zeng et al. (2010). H_2O_2 was visualized by diaminobenzidine (DAB) staining. Leaves were immersed and

vacuum-infiltrated with a solution of DAB in 50 mM phosphate buffer (pH 7.0) for 10 min and subsequently incubated at room temperature for 8 h in the dark. When brown spots appeared, the stained leaves were bleached by immersion in boiling ethanol (75%, v/v) to remove the pigments, and leaves were photographed by a digital camera. For localization of $^{\bullet}O_2^-$ in situ, leaves were vacuum-infiltrated with a solution containing 50 mM K-phosphate buffer (pH 6.4), 10 mM Na-azide, and 0.1% nitroblue tetrazolium (NBT) for 10 min and then left under white light (80 μmol m^{-2} s^{-1}) until the appearance of dark spots, characteristic of blue formazan precipitates. The subsequent steps were the same as for localization of H_2O_2.

2.10 Analysis of electrolyte leakage

Cell-membrane leakage rate was determined according to Lutts et al. (1996). Fresh leaves were immersed in double-distilled water for 1.5 h at room temperature, followed by a 30-min boiling treatment. The conductivity of a solution of leakage electrolytes before (EC1) and after boiling (EC2) was determined with a DDS-11C conductometer (Shanghai Dapu Instruments, Shanghai, China). The electrolyte leakage expressed in percentage (%) of total electrolytes, was calculated by using the formula: EL = (EC1/EC2) × 100 %.

2.11 Lipid peroxidation

Lipid peroxidation was estimated by determining the concentration of malondialdehyde (MDA) using the thiobarbituric acid (TBA) test (Draper and Hardly, 1990) with some modification. In brief, 0.1 g of fresh leaves was homogenized in 2 mL of 10% (w/v) TCA solution. The homogenate was centrifuged at 10,000 × *g* for 5 min, the supernatant was collected, and 1 ml of the supernatant was mixed with 1 ml of 0.67% (w/v) TBA prepared in 10% (w/v) TCA. The mixture was incubated in boiling water for 15 min, and the reaction was stopped in an ice bath. Samples were centrifuged again at 10,000 × *g* for 5 min, and the absorbance of the supernatant was read at 532, 600 and 450 nm for calculation of MDA content.

2.12 Statistical analysis

All data were average of four randomly selected replicates, and the results were expressed as

the mean ± standard error (SE). Statistical analysis was conducted by one-way ANOVA followed by a Duncan post-hoc test using Microsoft 2010 and SPSS Statistics 19 (IBM SPSS, Chicago, USA). Graphing was performed using SigmaPlot 12.5 software（Systat Software, San Jose, CA, USA）.

3. Results

3.1 Screening and identification of homozygous CHS-overexpression Arabidopsis thaliana

The *CHS* over-expression vector (*pCanGmyc-CHS* + EHA105) was constructed and identified (see Supplemental Material, Fig S1). The positive plasmid was transferred into *Arabidopsis thaliana* ecotype Columbia via the Agrobacterium-mediated floral dipping transformation method (Clough and Bent 1998). T_0 seeds were obtained from dipping flowers. T_0 seeds without successful transformation couldn't grow in kanamycin culture medium (Fig. 1A). T_0 lines were grown to produce T_1 seeds. T_1 seeds showed 3:1 separation characters in MS medium with kanamycin (Fig. 1B). T_1 lines were grown to produce T_2 seeds. Homozygous lines without character segregation were finally obtained with the kanamycin-resistance test (Fig. 1C). Three *CHS*-overexpression lines were generated for this study. The relative levels of expression of the *CHS* gene in the three overexpression lines were significantly increased compared with *Col*, ranging from 30-fold to 40-fold. But the relative expression level of the *CHS*-deletion line *tt4* was only 25% of *Col* (Fig. 1D). Immunoblotting analysis was consistent with the result of fluorescence quantitation PCR, showing that *CHS*-overexpression lines synthesized more CHS enzyme than WT (Fig. 1E).

3.2 Changes in anthocyanin accumulation in Arabidopsis thaliana under high-light treatment

Under normal growth conditions, the *CHS*-deletion line *tt4* showed weaker growth with fewer rosette leaves and earlier ageing than *Col* and *CHS*-overexpression lines. There was no obvious difference in the color of leaves between the five lines, and rosette leaves didn't turn red noticeably in a later growth period (Fig. 2A, B). Seedlings growing in compost under normal natural conditions for 25 days were transferred to HL. In the initial phase of HL treatment (up to three days of HL treatment), the five lines displayed normal green rosette leaves without turning

red. However, *tt4* showed leaf chlorosis and senility afterwards in HL treatment. Leaves of the four lines, with the exception of *tt4*, were deep red, and rosette leaves of *CHS*-overexpression lines were redder than *Col* (Fig. 2B). After 3 d of HL treatment, leaves of CHS-overexpression lines appeared red. On the sixth day of treatment, *tt4* began to become yellow first, while the others showed red leaves. HL resulted in ageing and mortality of tt4 leaves after 15 days of treatment. After a 20-day HL treatment, leaves of Col died but *CHS* lines survived until he twenty-fifth day (Fig. S2). Here, the absorption spectra (400 – 700 nm) of methanol-HCl extracts from leaves of the five lines were recorded. There were no obvious spectral absorption peaks of the anthocyanin extracts under normal illumination condition (Fig. 2C). However, there was an obvious difference in absorption spectrum in the three phenotypes after 12d under HL treatment. The contents of anthocyanins in *CHS*-overexpression lines were about 2-fold higher than that in the WT, but *tt4* still didn't show the typical absorption peak at 530 nm (Fig. 2D). Immunoblotting analysis on CHS enzyme also showed that the synthesis of CHS increased significantly after HL treatment of *Col* and the three overexpression lines (Fig. 1E).

3.3 Changes in relative expression of anthocyanin synthetic genes in Arabidopsis thaliana under HL treatment

There were obvious changes in anthocyanin accumulation in the five lines of *Arabidopsis thaliana* under HL treatment. We then explored the changes in relative expression level of anthocyanin synthetic genes, *CHS*, *DFR* and *ANS*, after HL treatment. Before HL treatment, the relative transcript levels of the *CHS* gene in two *CHS*-overexpression lines, *CHS2* and *CHS3*, were nearly 40-fold higher than in the WT, and in *CHS1* was 30-fold (Fig. 1D, 3A). But relative transcription levels of *DFR* and *ANS* in three *CHS*-overexpression lines were close to that of the WT (Fig. 3B, C). These results imply that the *CHS* lines were *CHS*-overexpression lines. On the contrary, the *CHS*-deletion line *tt4* showed a significantly lower transcription level of *CHS*, but much more expression of *DFR*, *ANS* genes than in *CHS*-overexpression lines and *Col* before HL treatment (Fig. 3); indeed, the expression of *DFR* was about 40-fold higher than in *CHS*-overexpression lines and *Col* (Fig. 3B). After 15 d under HL treatment, relative expression of *DFR* and *ANS* genes in all lines was significantly up-regulated, but not in the *CHS* gene. The relative expression levels of anthocyanin synthetic genes in *CHS*-overexpression lines were still

significantly higher than that of WT, while the *CHS* gene was down regulated compared with before treatment. The expression level of *CHS* and *DFR* genes in *tt4* were lower than in *Col*, but the expression level of *ANS* in *tt4* was higher than in Col (Fig. 3). The data are basically consistent with phenotype observation and anthocyanin contents (Fig. 2A, B).

3.4 Changes of chlorophyll fluorescence parameters in leaves of Arabidopsis thaliana under high-light treatment

We measured chlorophyll fluorescence parameters (including Fv/Fm, qP, Yield, ETR) of the five lines during HL treatment. There was no obvious difference in the four chlorophyll fluorescence parameters between the five lines before HL treatment. But with the extension of treatment time, chlorophyll fluorescence parameters of the five lines decreased at different rates (Fig. 4). Fv/Fm of *Arabidopsis* leaves of the five lines was about 0.81 to begin with. Fv/Fm of *Col* and *tt4* respectively dipped to 0.34 and 0.10, declining by 58.0% and 86.5% after a 12-day treatment, respectively. But *CHS* still remained at a relatively higher level, roughly declining by 30% (Fig. 4A). The decreasing trends of other chlorophyll fluorescence parameters (qP, Yield, ETR) were consistent with Fv/Fm: all those parameters decreased fastest in *tt4*, while those in the *CHS*-overexpression lines decreased more slowly (Fig. 4B, C, D). Chlorophyll fluorescence parameters of *CHS* lines were all higher than those of *Col* and *tt4*.

3.5 Changes in Rubisco protein content in leaves of Arabidopsis thaliana under high-light treatment

SDS-PAGE analysis showed that Rubisco contents in the five lines were higher before HL treatment than after. There were no significant differences between the five lines in Rubisco content without HL treatment (Fig. 5A). The Rubisco content of *tt4* decreased more drastically than in WT and *CHS*-overexpression lines (Fig. 5C). *CHS*-overexpression lines maintained the highest content among the five lines after HL treatment (Fig. 5A). To quantify these changes, TIFF files of the gel images were transferred for analysis by TotalLab TL120 (Nonlinear Dynamics Ltd., Newcastle, UK). Analysis data show that Rubisco contents in *CHS1*, *CHS2*, *CHS3*, *Col* and *tt4* declined by 48.7%, 52.9%, 50.1%, 65.6% and 97.7 %, respectively, after 12 d under HL treatment. The small subunit decreased more than the large subunit (Fig. 5D, E). Immunoblotting analysis on

the Rubisco large subunit (RL) was consistent with SDS-PAGE analysis (Fig. 5A, B).

3.6 Localization of the DAB-H_2O_2 and NBT-$^{\bullet}O_2^-$ compounds in tissues

Using diaminobenzidine (DAB) and nitroblue tetrazolium (NBT) histochemical staining, we detected the accumulation of H_2O_2 and $^{\bullet}O_2^-$ in leaves of the five lines. Some brown deposits, the product of reaction of H_2O_2 with DAB, could be observed in leaves after 12 d under HL treatment. The results suggest that the *tt4* mutant accumulated the most H_2O_2 followed by WT and then the *CHS*-overexpression lines according to color gradation and size of brown deposits (Fig. 6). The accumulation proportion of H_2O_2 were 60.1%, 9.0%, 7.3%, 43.0%, 87.0 % in *Col*, *CHS1*, *CHS2*, *CHS3* and *tt4*, respectively, determined by pixel counts in Adobe Photoshop 7.0 (Adobe Systems). In superoxide radical detection where the blue formazan precipitates are characteristic of a reaction of NBT with $^{\bullet}O_2^-$, we detected the corresponding accumulation of greater amounts of $^{\bullet}O_2^-$ with the H_2O_2 detection (Fig. 6). The percent staining relative to the total leaf area in Col, CHS1, CHS2, CHS3, and tt4 were 80.0%, 19.1%, 19.6%, 19.2%, 95.6%, respectively.

3.7 *Changes in relative membrane leakage and MDA in leaves of Arabidopsis thaliana under HL treatment*

Membrane permeability is a relevant index that reflects the degree of impaired membrane function. The higher the plasma membrane permeability, the more severe the cell membrane damage is (Shao et al., 2007). Before HL treatment, the cell membrane permeability was low in all the five lines. During the 15-d HL treatment, the cell membrane permeability of *tt4* mutant increased the fastest, while that of the *CHS*-overexpression lines remained at the lowest levels; cell membrane permeabilities of *tt4*, *Col*, *CHS3*, *CHS2*, *CHS1* were up to 80%, 58%, 39%, 38% and 35%, respectively (Fig. 7A). Membrane lipid peroxidation generates MDA (malondialdehyde) (Ding et al., 2010). Here, we detected MDA content in *Arabidopsis thaliana* rosette leaves during HL treatment. MDA contents of the five lines remained moderately low before HL treatment. As the HL treatment time increased, a rising trend of MDA content could be detected in the five lines, which showed a pattern very similar to that of cell membrane permeability (Fig. 7B).

4. Discussion

Overexpression transgenic lines constructed by the gene overexpression vector to transfect *Arabidopsis thaliana* is a common approach to studying gene functions. Here, we constructed a *CHS*-overexpression vector and transferred it into *Arabidopsis* ecotype Columbia (*Col*) (Fig S1). Finally, we generated three *CHS*-overexpression lines and named them *CHS1*, *CHS2*, *CHS3*, respectively. RT-PCR analysis showed that the relative expression of the *CHS* gene of these three overexpression lines was nearly 30-40 times higher than in *Col* (Fig. 1D). In order to further explore the role of anthocyanins in photoprotection, 25-day-old seedlings of *Arabidopsis* ecotype Columbia (*Col*), T-DNA insertion lines of *CHS* (*tt4*) and *CHS*-overexpression lines (*CHS1*, *CHS2*, *CHS3*) were treated under HL (200 μmol m^{-2} s^{-1}) to observe their physiological and biochemical responses to HL stress.

4.1 Anthocyanin accumulation enhances plant acclimation to HL

Under normal light conditions, *tt4* showed weaker growth and shorter survival time than the other two phenotypes, while there was no significant difference between the other four phenotypes (Fig. 2A). After 25-day-old seedlings were subjected to HL treatment for 12 d, *CHS1*, *CHS2* and *CHS3* appeared redder than *Col*, whereas rosette leaves of *tt4* did not turn red but rather appeared chlorotic. Almost all seedlings of *tt4* died after a 15-day treatment. Phenotype observations showed that upregulation of the *CHS* gene benefited *Arabidopsis* in its acclimation to HL stress (Fig. 2A, B). Spectrophotometric results suggest that the anthocyanins made the leaves appear red (Fig. 2C, D). In addition, immunoblotting analysis indicated that HL-induced synthesis of chalcone synthase was consistent with the observed phenotype (Fig. 1E). Therefore, we conclude that the *CHS*-overexpression lines, *CHS1*, *CHS2* and *CHS3*, synthesized more anthocyanins to resist HL stress by up-regulating *CHS* expression. By contrast, *tt4* showed the weakest resistance to HL stress, which resulted from down-regulation of *CHS* gene expression.

CHS, *DFR*, *ANS* are three important key enzymes in the early, middle and late stages of anthocyanin synthesis pathway, respectively. The expression level of *CHS* gene was very low in *tt4*, being only 25.6% of *Col*, whereas the expression levels of the *DFR* and *ANS* genes were nearly 40 times and 10 times more than Col, respectively (Fig. 3). *tt4* might have up-regulated midstream and downstream genes to counteract the negative impact of the lack of *CHS* expression.

We tend to call it a feedback-compensatory effect. After HL treatment, expression levels of *CHS*, *DFR*, *ANS* gene in *Col* were significantly up-regulated, especially the *DFR* and *ANS* genes. This implies that HL treatment would induce accumulation of anthocyanins by up-regulating middle- and late-biosynthetic genes, results which are similar to those of Xu et al. (2017). In addition, the *CHS*, *DFR* and *ANS* gene expression levels of *CHS*-overexpression lines were significantly higher than in *Col*, which illustrates that overexpression of the *CHS* gene enabled the up-expression of *CHS*, *DFR*, *ANS* and a substantial accumulation of anthocyanins under HL. By contrast, the expression of *CHS* and *DFR* genes in *tt4* was significantly lower than in *Col*, though there was no statistical significance in the case of the *ANS* gene; this indicates that interfering with *CHS* gene expression not only affected the *CHS* gene but also others involved in anthocyanin biosynthesis.

4.2 Anthocyanins partly protect the photosynthetic apparatus from HL stress

If plants are grown in an HL environment with another stress, the efficiency of CO_2 fixation in chloroplasts and the utilization of light energy would be reduced, resulting in excess light energy that leads to photodamge of the photosynthetic apparatus (Yang et al., 2002). Chlorophyll fluorescence quenching analysis is a rapid and non-invasive approach to measure photosynthetic function of leaves (Genty et al., 1989; Schreiber et al., 1995). It has been widely used in many fields of studies, such as photosynthetic mechanisms, plant stress physiology, prediction of potential crop yield by estimating activity of Photosystem II (PSII) and the partitioning of light energy between heat dissipation and photosynthetic electron transport (Demmig-Adams and Adams, 1996; Krall and Edwards, 1992). We analyzed the activity of PS II in the five lines by chlorophyll fluorescence analysis and the results show significant diversities among the three phenotypes after HL stress. Fv/Fm of all lines decreased to different degrees after HL treatment. *CHS*1, *CHS2* and *CHS3* maintained higher Fv/Fm than the other two lines, of which *tt4* showed the greatest decrease in Fv/Fm. The results indicate that *tt4* suffered the most severe photoinhibition, while the large accumulation of anthocyanins partly relieved photoinhibition in *CHS*-overexpression lines (Fig. 4A).

The parameter qP indicates the redox state of primary quinone electron acceptor of PSII (Q_A) and, therefore, the number of open PSII reaction center traps. qP decreased sharply in the

anthocyanin-deficient mutant after HL stress, indicating that number of open PSII reaction centers badly decreased and, therefore, the ability of *tt4* to fix CO_2 badly declined. But *CHS1*, *CHS2* and *CHS3* still maintained high electron transport activity of PSII (Fig. 4D). Yield and ETR presented a similar pattern as Fv/Fm and qP did. The results suggest that the photochemical conversion efficiency of *tt4* was severely affected by HL stress, but that anthocyanins in the other lines partly ameliorated the photodamage to the photosynthetic apparatus (Fig. 4B, C).

Ribulose-1, 5-bisphosphate carboxylase / oxygenase (Rubisco; EC 4.1.1.39) is not only the first key enzyme in net photosynthetic CO_2 assimilation and photorespiratory carbon oxidation, but also a storage protein in plants (Andersson and Backlund, 2008; Hartman and Harpel, 1994). Land plants allocate as much as 50% of their leaf nitrogen to Rubisco, making this single enzyme the most abundant protein in the world (Spreitzer and Salvucci 2002). The activity and content of Rubisco are affected by various environmental factors, such as illumination, CO_2 concentration and temperature. The decrease in Rubisco content is a strategy by which plants acclimate to the environment with high light intensity, high CO_2 level, low temperature and other stresses (Makino et al., 1997). In this study, SDS-PAGE image analysis and protein immunoblotting revealed that there was no significant difference in the content of total Rubisco, nor in the separate large and small subunits of Rubisco, among the three phenotypes before HL treatment. After 12 days in HL, however, their Rubisco contents all greatly declined, especially in *tt4* (Fig. 5). The results indicate that anthocyanins could maintain activity and integrity of enzymes related to photosynthesis. Thus, this is another way in which anthocyanins decreased the degree of damage to photosynthetic apparatus under HL.

4.3 Anthocyanins ameliorate the damage of the membranes system by ROS

Reactive oxygen species (ROS) are unavoidable by-products of cellular metabolism in plants under environmental stress. ROS mainly cause peroxidation of membrane lipids, so membranes including photosynthetic membranes are subject to oxidative damage (Chia et al., 1981; Babbs and Griffin, 1989). Thus, the content of malondialdehyde (MDA) which is the end product of membrane lipid peroxidation, and cell membrane permeability can both reflect the degree of damage to the cell membrane. The higher content of MDA and greater cell membrane

permeability indicate the more serious damage of the cell membrane and the accumulation of more free radicals. In the present study, the content of MDA and cell membrane permeability of three phenotypes rapidly increased after HL treatment. These two parameters in the *tt4* line increased most quickly, followed by *Col* and then the *CHS*-overexpression lines (Fig. 7). Our results show that *CHS*-overexpression lines maintained great stability of the membrane system due to abundant anthocyanins. By contrast, cell membranes of the anthocyanin-deficient mutant (*tt4)* suffered the most serious damage, resulting in exacerbation of electrolyte leakage.

4.4 Anthocyanins enhance acclimation of plant to HL via both antioxidation and light attenuation

If light intensity is higher than the light saturation point (LSP), light that cannot be used or dissipated safely would induce photoinhibition in plants and decrease the photosynthetic rate (Shulaev and Oliver 2006). Photoinhibition is generally accompanied by the generation and accumulation of ROS. Oxidative stress induced by ROS seriously damages the photosynthetic reaction center (PSI and PSII), photosynthetic pigments and cell membrane systems. The above results demonstrate that anthocyanins could partly protect the photosynthetic apparatus from damage by HL and lighten the damage of ROS to the membrane systems. We have localized ROS in the tissue of rosette leaves, and the results show that the five lines displayed various degrees of accumulation of H_2O_2 and $^{\bullet}O_2^-$. Generally, chloroplasts, peroxisome and mitochondria are the principal sites of ROS production (Hossain and Fujita, 2012). $^{\bullet}O_2^-$ cannot readily permeate the tonoplast, and it is rapidly protonated to form hydroperoxyl radical, or dismutated by SOD to H_2O_2. (Takahashi and Asada, 1997; Yamasaki 1997; Neill and Gould, 2003). H_2O_2 is a longer-lived ROS, which tends to be transported and detoxified in the vacuole (Yamasaki 1997). Many of the enzymes in the *Arabidopsis* anthocyanin biosynthetic pathway participate in the formation of multienzyme complexes which are anchored in the cytoplasmic face of the endoplasmic reticulum (ER) (Grotewold 2006). Anthocyanins synthetized in the cytoplasm then are mostly transported and kept in the vacuole (Klein et al., 1996). Thus, anthocyanins lighten the damage of ROS by scavenging and removing the most ROS. Anthocyanins can scavenge ROS possibly because of their special chemical structure: anthocyanins are rich in aromatic rings and conjugated double bonds, which make it easy to exchange a hydrogen atom or electron with a free radical, thereby stabilizing free radicals for delocalization (Zhang et al., 2015). Peng et al. (2006)

demonstrated that purple rice leaves rich in anthocyanins could partly resist exogenous photooxidative damage. Lee and Gould (2002) concluded that anthocyanins scavenge ROS such as H_2O_2 and $^{\bullet}O_2^-$, and that the antioxidative capacity of anthocyanins is about 4-fold higher than that of α-tocopherol.

As we can see from Figure 2, anthocyanins could absorb light of specific wavelengths from 400 nm to 600 nm. Light reaching mesophyll cells is intercepted by anthocyanins, especially green light. The characteristic light-absorbing property of anthocyanins restricts the absorption of green light to the mesophyll, though it has little effect on the absorption of red and blue light used in photosynthesis (Gould at al., 2002). This may be why plants adopted this pigment as a light screen, under HL treatment or other stresses. Anthocyanins attenuate part of luminous energy to reduce excess photons so that plants can partly maintain their normal metabolism. Noticeably, anthocyanins provide an efficient mechanism to limit the generation of $^{\bullet}O_2^-$ without impacting substantially on the action spectrum for photosynthesis (Neill and Gould, 2003). It is also the reason why CHS-overexpression lines accumulated less ROS (Fig. 6). Previous studies have also demonstrated that anthocyanins reduce excessive light reaching chloroplasts, so the damage to the photosynthetic apparatus by HL is reduced and the photosynthetic enzymes are maintained at high integrity and activity (Gould et al., 2002; Albert 2009). Anthocyanins in leaves of eggplant absorb and intercept light in the wavelength range 500-600 nm (yellow-green light). In this way, they protect PSI and PSII, moderate the reduction state of electron transporters, alleviate the pressure on the thermal dissipation mechanism and maintain the balance of light reactions and carbon fixation reactions (Xue et al., 2009). Thus, photoprotection by anthocyanins is derived not only from their antioxidative function, but also their absorption of light.

In general, the accumulation of anthocyanins is positively correlated with the light intensity. The higher light intensity is, the more anthocyanins are synthesized. In addition, *CHS1*, *CHS2* and *CHS3* accumulated more anthocyanins through *CHS* gene overexpression. Adaptability to HL of *CHS*-overexpression line showed superiority compared with *Col*, while *tt4* exhibited high sensitivity to HL. Anthocyanins play an important part in photoprotection. On the one hand, anthocyanins could modulate the ROS level, and lighten the damage of peroxidation caused by HL stress. On the other hand, anthocyanins could absorb part of the light energy; thus, excess light is

lessened. Anthocyanins could relieve photoinhibition, protect photosynthetic enzymes, and mitigate the degree of damage under HL to plant photosynthetic apparatus. However, there is still growing debate over which of the two anthocyanin functions is more important. To resolve the dispute, future experiments will have to address the relative contributions of the two anthocyanin functions to photoprotection.

Acknowledgements

This work was funded by the National Key R&D Program of China (2017YFC1200105) and Guangdong Province Natural Science Foundation (2017A030313167, 2015A030311023). The study was also supported by the National Natural Science Foundation of China (31570398), Science and Technology Program of Guangzhou (20170701257) and Yang Cheng Scholar Program (10A040G).

References

Albert, N.W., Lewis, D.H., Zhang, H., Irving, L.J., Jameson, P.E., Davies, K.M., 2009. Light-induced vegetative anthocyanin pigmentation in Petunia. J. Exp. Bot. 60, 2191-2202.

Andersen, Ø.M., Jordheim, M., 2005. The Anthocyanins. In: Andersen, Ø.M., Markham, K.R., (Ed.), Flavonoids: Chemistry, Biochemistry and Applications. CRC Press, Boca Raton, FL, pp. 471-552.

Andersson, I., Backlund, A., 2008. Structure and function of Rubisco. Plant Physiol. Biochem. 46, 275-291.

Babbs, C.F., Griffin, D.W., 1989. Scatchard analysis of methane sulfinic acid production from dimethyl sulfoxide: a method to quantify hydroxyl radical formation in physiologic systems. Free Radical Bio. Med. 6, 493-503.

Barczak-Brzyżek, A.K., Kiełkiewicz, M., Gawroński, P., Kot, K., Filipecki, M., Karpińska, B. 2017. Cross-talk between high light stress and plant defence to the two-spotted spider mite in Arabidopsis thaliana. Exp. Appl. Acarol. 1-13.

Catalá, R., Medina, J., Salinas, J., 2011. Integration of low temperature and light signaling during cold acclimation response in arabidopsis. Proc. Natl. Acad. Sci. USA 108, 16475-80.

Chen, T.W., Stützel, H., Kahlen, K. 2017. High light aggravates functional limitations of cucumber canopy photosynthesis under salinity. Ann. Bot-london

Chia, L.S., Thompson, J.E., Dumbroff, E.B., 1981. Simulation of the effects of leaf senescence on membranes by treatment with paraquat. Plant Physiol. 67, 415-420.

Clough, S.J., Bent, A.F., 1998. Floral dip: a simplified method for Agrobacterium-mediated transformation of Arabidopsis thaliana. Plant J. 16, 735

Genty, B., Briantais, J.M., Baker, N.R., 1989. The relationship between the quantum yield of photosynthetic electron transport and quenching of chlorophyll fluorescence. BBA-Gen. Subjects 990, 87-92.

Demmig-Adams, B., Adams Iii, W.W., 1992. Photoprotection and other responses of plants to high light stress. Annu. Rev. Plant Biol. 43, 599-626.

Demmig-Adams, B., Adams, W.W., 1996. The role of xanthophyll cycle carotenoids in the protection of photosynthesis. Trends Plant Sci. 1, 21-26.

Ding, W., Song, L., Wang, X., Bi, Y., 2010. Effect of abscisic acid on heat stress tolerance in the

calli from two ecotypes of Phragmites communis. Biol. Plantarum 54, 607-613.

Donahue, J.L., Okpodu, C.M., Cramer, C.L., Grabau, E.A., Alscher, R.G., 1997. Responses of antioxidants to paraquat in pea leaves (relationships to resistance). Plant Physiol. 113, 249-257.

Draper, H.H., Hadley, M., 1990. Malondialdehyde determination as index of lipid Peroxidation. Method Enzymol. 186, 421-431.

Faseela, P., Puthur, J.T., 2016. Chlorophyll a, fluorescence changes in response to short and long term high light stress in rice seedlings. Indian J. Plant physiol. 22, 1-4.

Genty, B., Briantais, J.M., Baker, N.R., 1989. The relationship between the quantum yield of photosynthetic electron transport and quenching of chlorophyll fluorescence. BBA-Gen. Subjects 990, 87-92.

Gläßgen, W.E., Rose, A., Madlung, J., Koch, W., Gleitz, J., Seitz, H.U., 1998. Regulation of enzymes involved in anthocyanin biosynthesis in carrot cell cultures in response to treatment with ultraviolet light and fungal elicitors. Planta 204, 490-498.

Gould, K.S., McKelvie, J., Markham, K.R., 2002. Do anthocyanins function as antioxidants in leaves? Imaging of H_2O_2 in red and green leaves after mechanical injury. Plant Cell Environ. 25, 1261-1269.

Gray, G.R., Hope, B.J., Qin, X., Taylor, B.G., Whitehead, C.L., 2003. The characterization of photoinhibition and recovery during cold acclimation in Arabidopsis thaliana using chlorophyll fluorescence imaging. Physiol. Plantarum 119, 365-375.

Grotewold, E., 2006. The genetics and biochemistry of floral pigments. Annu. Rev. Plant Biol. 57, 761-780.

Hartman, F.C., Harpel, M.R., 1994. Structure, function, regulation, and assembly of D-ribulose-1, 5-bisphosphate carboxylase/oxygenase. Annu. Rev. Biochem. 63, 197-232.

Hossain, M.A., Fujita, M., 2012. Regulatory role of components of ascorbate-glutathione (AsA-GSH) pathway in plant tolerance to oxidative stress. In: Anjum, N.A., Umar, S., Ahmad, A., (Ed.), Oxidative stress in plants: causes, consequences and tolerance, IK International Publishing House Pvt. Ltd., INDIA, pp. 81-147.

Howe, G., Mets, L., Merchant, S., 1995. Biosynthesis of cytochrome f in Chiamydomonas reinhardtii: analysis of the pathway in gabaculine-treated cells and in the heme attachment

mutant B6. Mol. Gen. Genet. 246, 156-165.

Hughes, N.M., Neufeld, H.S., Burkey, K.O., 2005. Functional role of anthocyanins in high-light winter leaves of the evergreen herb Galax urceolata. New Phytol. 168, 575-587.

Hughes, N.M., Smith, W.K., 2007. Attenuation of incident light in *Galax urceolata* (Diapensiaceae): concerted influence of adaxial and abaxial anthocyanic layers on photoprotection. Am. J. Bot. 94, 784-790.

Karageorgou, P., Manetas, Y., 2006. The importance of being red when young: anthocyanins and the protection of young leaves of *Quercus coccifera* from insect herbivory and excess light. Tree Physiol. 26, 613-621.

Klein, M., Weissenböck, G., Dufaud, A., Gaillard, C., Kreuz, K., Martinoia, E., 1996. Different energization mechanisms drive the vacuolar uptake of a flavonoid glucoside and a herbicide glucoside. Journal of Biological Chemistry, 271, 29666-29671.

Krall, J.P., Edwards, G.E., 1992. Relationship between photosystem II activity and CO_2 fixation in leaves. Physiol. Plantarum 86, 180-187.

Krause, G.H., Weis, E., 1988. The photosynthetic apparatus and chlorophyll fluorescence. An introduction. In: Lichtenthaler, H.K. (Ed.) Applications of Chlorophyll Fluorescene in Photosynthesis Research, Stress Physiology, Hydrobiology and Remote Sensing. Springer Netherlands, pp. 3-11.

Kootstra, A., 1994. Protection from UV-B-induced DNA damage by flavonoids. Plant. Mol. Biol. 26, 771-774.

Lee, D.W., Gould, K.S., 2002. Anthocyanins in leaves and other vegetative organs: an introduction. Adv. Bot. Res. 37, 1-16.

Livak, K.J., Schmittgen, T.D., 2001. Analysis of relative gene expression data using real-time quantitative PCR and the $2^{-\Delta\Delta CT}$ method. Methods 25, 402-408.

Lu, T., Meng, Z., Zhang, G., Qi, M., Sun, Z., Liu, Y., Li, T. 2017. Sub-high Temperature and High Light Intensity Induced Irreversible Inhibition on Photosynthesis System of Tomato Plant (Solanum lycopersicum L.). Front. Plant sci. 8.

Lutts, S., Kinet, J.M., Bouharmont, J., 1996. NaCl-induced senescence in leaves of rice (*Oryza sativa L.*) cultivars differing in salinity resistance. Ann. Bot. 78, 389-398.

Makino, A., Shimada, T., Takumi, S., Kaneko, K., Matsuoka, M., Shimamoto, K., Nakano, H.,

Yamamoto, N., 1997. Does decrease in ribulose-1, 5-bisphosphate carboxylase by antisense RbcS lead to a higher N-use efficiency of photosynthesis under conditions of saturating CO_2 and light in rice plants?. Plant Physiol. 114, 483-491.

Merzlyak, M.N., Chivkunova, O.B., Solovchenko, A.E., Naqvi, K.R. 2008. Light absorption by anthocyanins in juvenile, stressed, and senescing leaves. J. Exp. Bot. 59, 3903-3911.

Mittler, R., 2002. Oxidative stress, antioxidants and stress tolerance. Trends Plant Sci. 7, 405-410..

Neill, S.O., Gould, K.S., 2003. Anthocyanins in leaves: light attenuators or antioxidants?. Funct. Plant Biol. 30, 865-873.

Olaizola, M., Duerr, E.O., 1990. Effects of light intensity and quality on the growth rate and photosynthetic pigment content of *Spirulina platensis*. J. Appl. Phycol. 2, 97-104.

Oh, J.E., Kim, Y. H., Kim, J.H., Ye, R.K., Lee, H. 2011. Enhanced level of anthocyanin leads to increased salt tolerance in arabidopsis pap1-d, plants upon sucrose treatment. J. Korean soc. Appl. Bi. 54, 79-88.

Oren-Shamir, M., 2009. Does anthocyanin degradation play a significant role in determining pigment concentration in plants?. Plant Sci. 177, 310-316.

Peng, C., Lin, Z., Lin, G., Chen, S., 2006. The anti-photooxidation of anthocyanins-rich leaves of a purple rice cultivar. Sci. China Ser. C: Life Sci. 49, 543-551.

Pietrini, F., Iannelli, M.A., Massacci, A., 2002. Anthocyanin accumulation in the illuminated surface of maize leaves enhances protection from photo-inhibitory risks at low temperature, without further limitation to photosynthesis. Plant Cell Environ. 25, 1251-1259

Rice-Evans, C., Miller, N., Paganga, G., 1997. Antioxidant properties of phenolic compounds. Trends Plant Sci. 2, 152-159.

Romero-Puertas, M.C., Rodríguez-Serrano, M., Corpas, F.J., Gomez, M.D., Del Rio, L.A., Sandalio, L.M., 2004. Cadmium-induced subcellular accumulation of $O_2^{\cdot-}$ and H_2O_2 in pea leaves. Plant Cell Environ. 27, 1122-1134.

Rubin, G., Tohge, T., Matsuda, F., Saito, K., Scheible, W.R., 2009. Members of the LBD family of transcription factors repress anthocyanin synthesis and affect additional nitrogen responses in Arabidopsis. Plant Cell 21, 3567-3584.

Schreiber, U., Schliwa, U., Bilger, W., 1986. Continuous recording of photochemical and non-photochemical chlorophyll fluorescence quenching with a new type of modulation

fluorometer. Photosynth Res. 10, 51-62.

Schreiber, U.B.W.N., Bilger, W., Neubauer, C., 1995. Chlorophyll fluorescence as a nonintrusive indicator for rapid assessment of in vivo photosynthesis. In: Schulze, E.D., Caldwell, M.M. (Eds.), Ecophysiology of photosynthesis. Springer Berlin Heidelberg, pp. 49-70.

Schumann, T., Paul, S., Melzer, M., Doermann, P., Jahns, P. 2017. Plant Growth under Natural Light Conditions Provides Highly Flexible Short-Term Acclimation Properties toward High Light Stress. Front. Plant sci. 8.

Shao, L., Shu, Z., Sun, S.L., Peng, C.L., Wang, X.J., Lin, Z.F., 2007. Antioxidation of anthocyanins in photosynthesis under high temperature stress. J. Integr. Plant Biol. 49, 1341-1351.

Shulaev, V., Oliver, D.J., 2006. Metabolic and proteomic markers for oxidative stress. New tools for reactive oxygen species research. Plant Physiol. 141, 367-372.

Singh, A.S., Jones, A.M.P., Shukla, M.R., Saxena, P.K., 2017. High light intensity stress as the limiting factor in micropropagation of sugar maple (Acer saccharum Marsh.). Plant Cell Tiss. Org. 129, 209-221.

Spreitzer, R.J., Salvucci, M.E., 2002. Rubisco: structure, regulatory interactions, and possibilities for a better enzyme. Annu. Rev. Plant Biol. 53, 449.

Steyn, W.J., Wand, S.J.E., Holcroft, D.M., Jacobs, G., 2002. Anthocyanins in vegetative tissues: a proposed unified function in photoprotection. New Phytol. 155, 349-361.

Takahashi, M.A., Asada, K., 1983. Superoxide anion permeability of phospholipid membranes and chloroplast thylakoids. Arch. Biochem. Biophys. 226, 558-566.

Tanaka, Y., Sasaki, N., Ohmiya, A., 2008. Biosynthesis of plant pigments: anthocyanins, betalains and carotenoids. Plant J. 54, 733-749.

Teng, S., Keurentjes, J., Bentsink, L., Koornneef, M., Smeekens, S., 2005. Sucrose-specific induction of anthocyanin biosynthesis in Arabidopsis requires the MYB75/PAP1 gene. Plant Physiol. 139, 1840-1852.

Tian, Y., Zheng, G.Y., Zhang, H.H., Xu, N., Wang, J., Sun, G.Y., 2013. Effects of light intensity and temperature on chlorophyll fluorescence in leaves of basil seedlings. Pratacultural Sci. 30, 1561-1568.

Wade, H.K., Sohal, A.K., Jenkins, G.I., 2003. Arabidopsis ICX1 is a negative regulator of several

pathways regulating flavonoid biosynthesis genes. Plant Physiol. 131, 707-715.

Wang, J., Guo, M., Li, Y., Wu, R., Zhang, K. 2017. High‐throughput Transcriptome Sequencing Reveals the Role of Anthocyanin Metabolism in Begonia semperflorens Under High Light Stress. Photochem. Photobiol.

Xu, Z., Mahmood, K., Rothstein, S.J., 2017. ROS Induces Anthocyanin Production Via Late Biosynthetic Genes and Anthocyanin Deficiency Confers the Hypersensitivity to ROS-generating Stresses in Arabidopsis. Plant Cell Physiol. pcx073.

Xue. Z.J., Gao. Z.K., Wang. M., Zhong. C.F., Gao. R.F., 2009. Protective action on photosynthetic apparatus by purple anthocyanin in the epidermal cells of eggplant (*Solanum melongena L.*) leaves. Acta Ecologica Sinica 29, 1374-1381.

Yamasaki, H., Sakihama, Y., Ikehara, N., 1997. Flavonoid-peroxidase reaction as a detoxification mechanism of plant cells against H_2O_2. Plant Physiol. 115, 1405-1412.

Yang, G.D., Zhu, Z.J., Ji, Y.M., 2002. Effect of light intensity and magnesium deficiency on chlorophyll fluorescence and active oxygen in cucumber leaves. Plant Nutr. Fertil. Sci. 8, 115-118.

Yu, X., Zhou, R., Wang, X., Kjær, K.H., Rosenqvist, E., Ottosen, C.O., Chen, J., 2016. Evaluation of genotypic variation during leaf development in four *Cucumis* genotypes and their response to high light conditions. Environ. Exp. Bot. 124, 100-109.

Zeng, L.D., Li, M., Chow, W.S., Peng, C.L., Susceptibility of an ascorbate-deficient mutant of Arabidopsis to high-light stress. Photosynthetica, 1-6.

Zeng, X.Q., Chow, W.S., Su, L.J., Peng, X.X., Peng, C.L., 2010. Protective effect of supplemental anthocyanins on Arabidopsis leaves under high light. Physiol. Plantarum 138, 215-225.

Zhang, Q., Su, L.J., Chen, J.W., Zeng, X.Q., Sun, B.Y., Peng, C.L., 2012. The antioxidative role of anthocyanins in Arabidopsis under high-irradiance. Biol. Plantarum 56, 97-104.

Zhang, T.J., Chow, W.S., Liu, X.T., Zhang, P., Liu, N., Peng, C.L., 2016. A magic red coat on the surface of young leaves: anthocyanins distributed in trichome layer protect Castanopsis fissa leaves from photoinhibition. Tree Physiol. 36, 1296-1306.

Zhang, T.J., Zheng, J., Yu, Z.C., Gu, X.Q., Tian, X.S., Peng, C.L., Chow, W.S. 2017. Variations in photoprotective potential along gradients of leaf development and plant succession in subtropical forests under contrasting irradiances. Environ Exp Bot.

http://dx.doi.org/10.1016/j.envexpbot.2017.07.016

Zhang, Y., De Stefano, R., Robine, M., Butelli, E., Bulling, K., Hill, L., Rejzek. M., Martin. C., Schoonbeek, H.J., 2015. Different reactive oxygen species scavenging properties of flavonoids determine their abilities to extend the shelf life of tomato. Plant Physiol. 169, 1568-1583.

Fig. 1

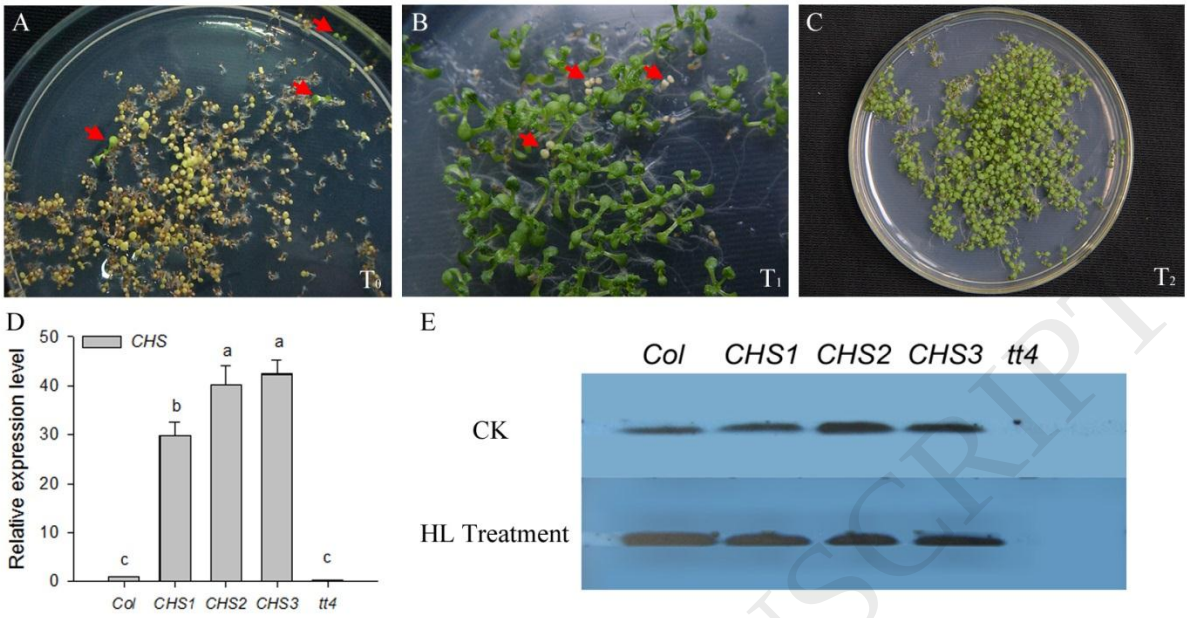

Fig. 1 Screening and identification of homozygous *CHS*-overexpression *Arabidopsis thaliana*. (A-C) Transgenic *Arabidopsis thaliana* plants (*pCanGmyc-CHS*) on 1×MS + 50 mg/L Kan culture medium plate. (A) T_0 seeds in culture medium plate with 50 mg/L Kan. Red arrows indicate green T_0 seedings of successful transformation. (B) T_1 seeds in culture medium plate with 50 mg/L Kan. T_1 seedings showed 3:1 characters separation in MS medium with kanamycin. Red arrows indicate recessive homozygous T_1 seedings. (C) Homozygous T_2 seeds without characters separation in culture medium plate with Kan. (D) Indentification of *CHS*-overexpression lines by qRT-PCR of CHS gene. Data are mean ± SE (n = 4). Different letters above bars indicate statistical significance ($P < 0.05$). (E) Identification of *CHS*-overexpression lines by immunoblotting analysis of CHS enzyme. The first row show the immunoblotting of CHS enzyme in leaves of *Arabidopsis thaliana* (*Col*, *CHS1*, *CHS2*, *CHS3*, *tt4*) before HL treatment (CK), and the second row show that of *Arabidopsis thaliana* under HL treatment for 12d.

Fig. 2

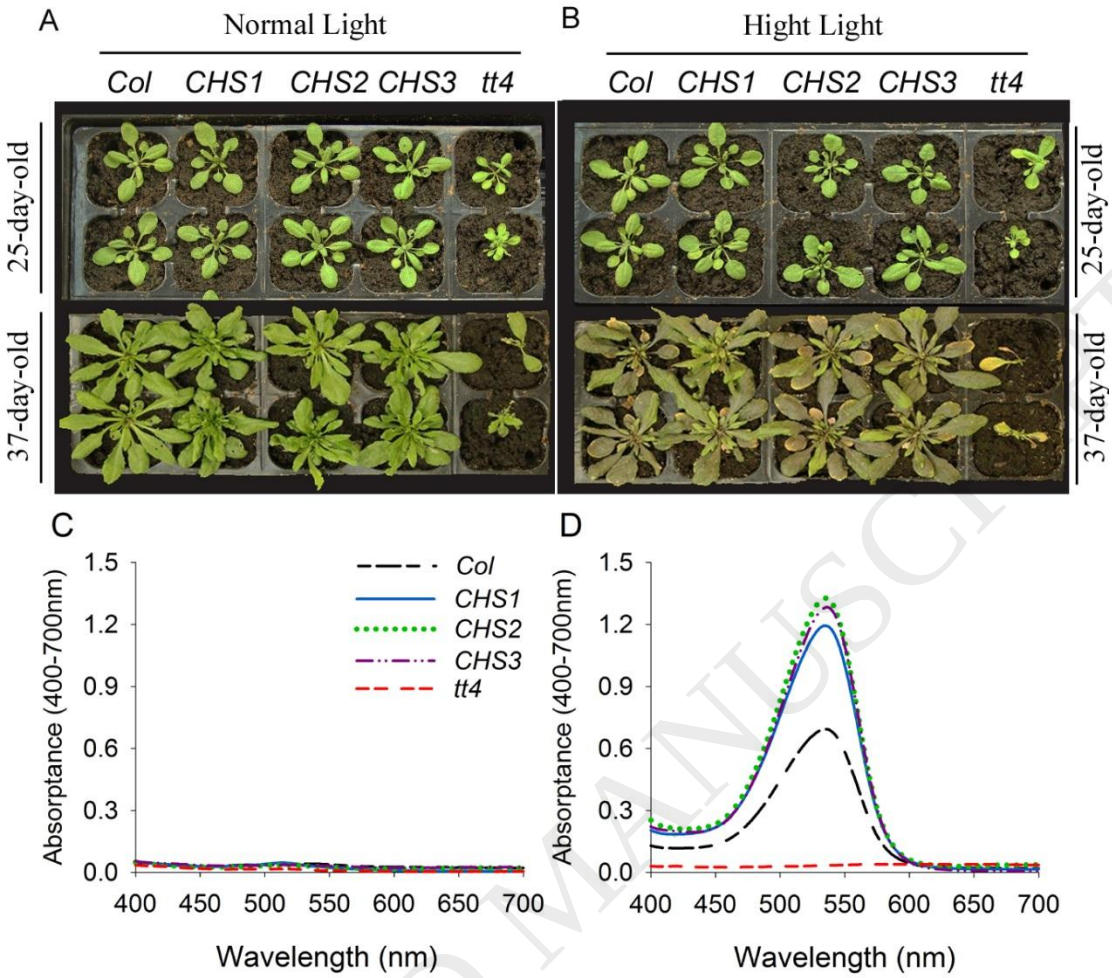

Fig.2 Different accumulation levels of anthocyanins in *Arabidopsis*. (A) Changes of leaf phenotype in normal light (PPFD 100 μmol m^{-2} s^{-1}). (B) Changes of leaves phenotype in HL (PPFD 200μmol m^{-2} s^{-1}). 25-day-old seedlings (the 1st day of HL treatment) are in the first two rows. 37-day-old seedings (the 12th day of HL treatment) are in the 3rd and 4th row. The different absorbance spectra of anthocyanin in the five lines on the 1st (C) and 12th (D) day of HL treatment (n = 4).

Fig. 3

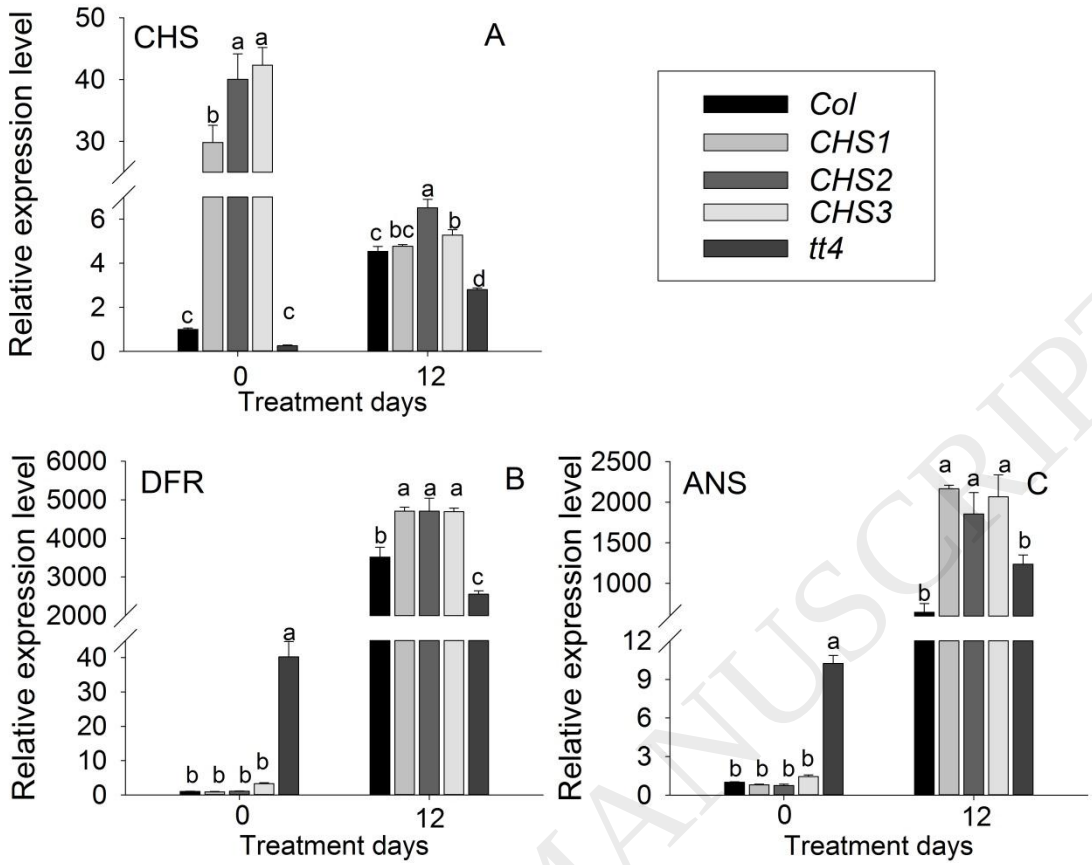

Fig.3 Expression analysis of anthocyanins-related genes [*CHS* (A), *DFR* (B), *ANS* (C)] in mutants and *Col* before HL treatment or after 12 days of HL (200 μmol m^{-2} s^{-1}). Data are mean ± SE (n = 4). Different letters above bars indicate statistical significance ($P < 0.05$).

Fig. 4

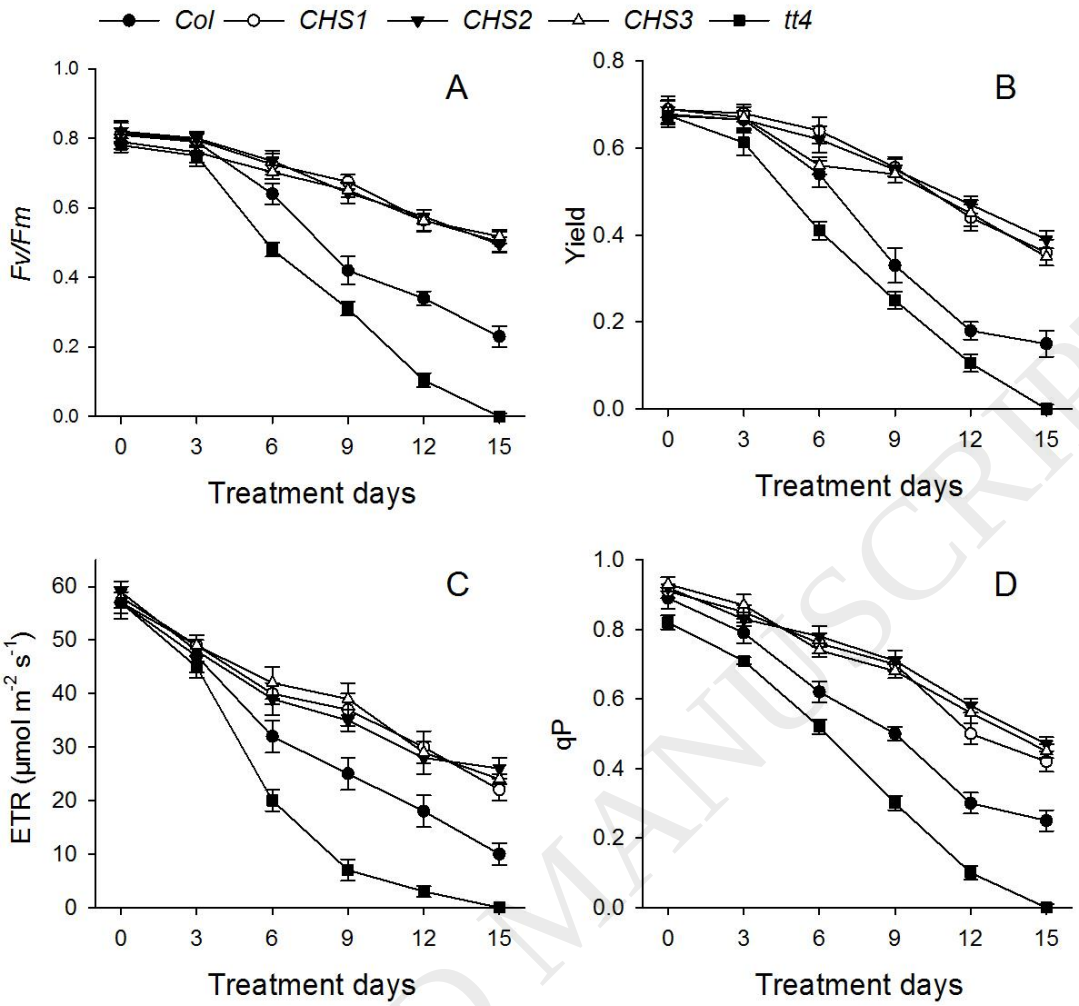

Fig. 4 Changes of chlorophyll fluorescence parameters -- Fv/Fm (A), Yield (B), ETR (C) and qP (D) in rosette leaves of *Arabidopsis thaliana* (*Col*, *CHS1*, *CHS2*, *CHS3*, *tt4*) under HL treatment (200 μmol m^{-2} s^{-1}). The measurement photon flux density was 200 μmol m^{-2} s^{-1}. Data are mean ± SE (n = 4).

Fig. 5

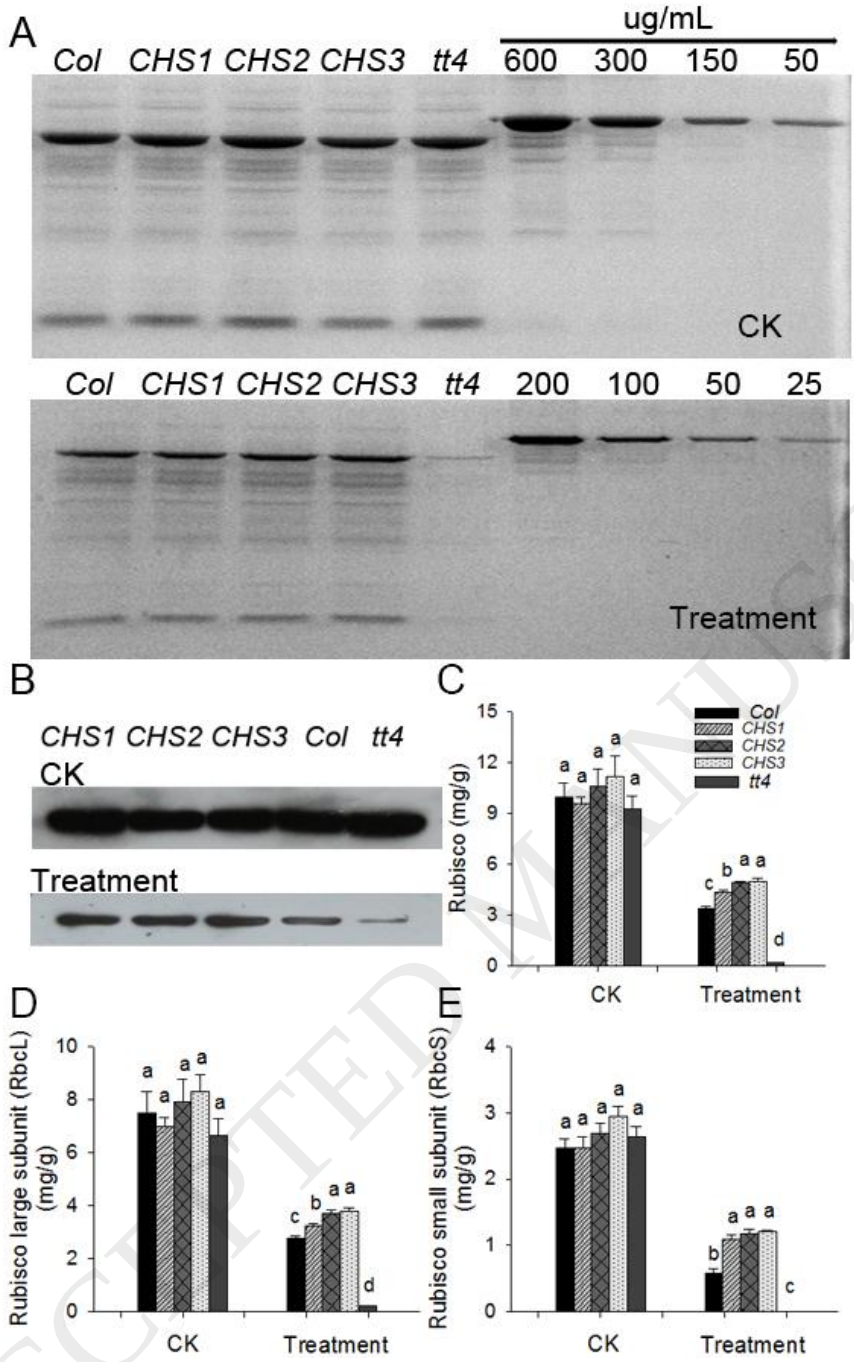

Fig. 5 Decrease in Rubisco protein content in leaves of *Arabidopsis thaliana* (*Col, CHS1, CHS2, CHS3, tt4*). (A) Rubisco large subunit (RbcL, 55 kDa) and small subunit (RbcS, 15 kDa) were separated by 12.5% SDS-PAGE. The polypeptides were visualized by Coomassie Brilliant Blue R-250 staining. The loading protein sample of first SDS-PAGE gel are soluble proteins in leaves of *Arabidopsis thaliana* (*Col, CHS1, CHS2, CHS3, tt4*) before HL treatment (CK), and the second gel are soluble proteins in leaves of *Arabidopsis thaliana* under HL treatment for 12d. (B) Immunoblotting of RbcL. (C-E) Contents of total Rubisco (RbcL + RbcS) (C), Rubisco large subunit (RbcL) (D), and Rubisco small subunit (RbcS) (E) was estimated by using bovine serum albumin (BSA, 67 kDa) as the standard. Data are mean ± SE (n = 4). Different letters above bars indicate statistical significance ($P < 0.05$).

Fig. 6

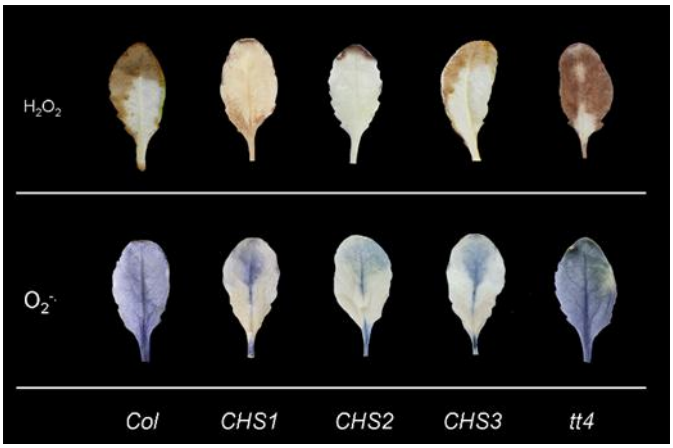

Fig. 6 Diaminobenzidine (DAB) and nitroblue tetrazolium (NBT) staining showed the accumulation of H_2O_2 and $^{\bullet}O_2^-$ in leaves of *Arabidopsis thaliana* (*Col*, *CHS1*, *CHS2*, *CHS3*, *tt4*) after 12 days exposure to HL (200 μmol m^{-2} s^{-1}).

Treatment days Treatment days

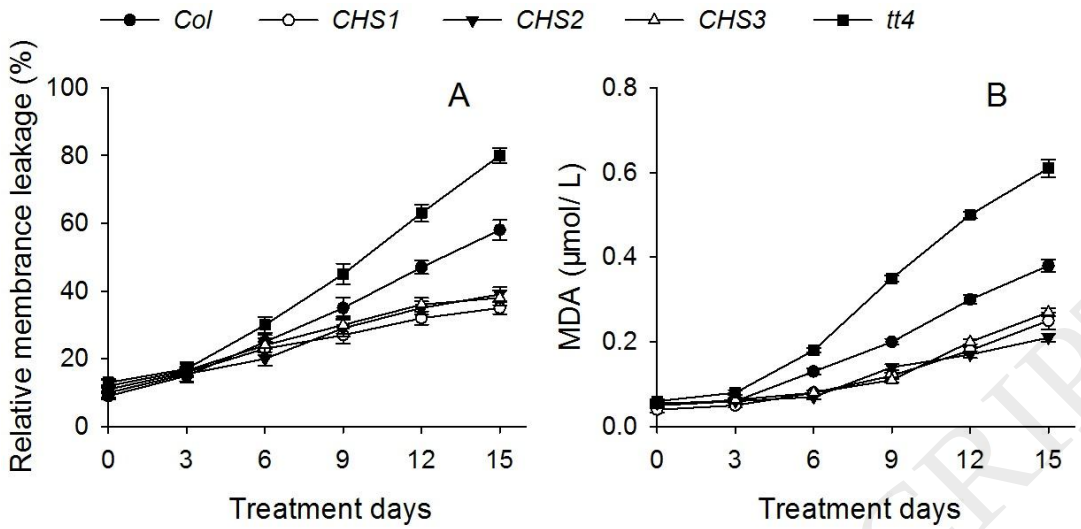

Fig. 7 Changes in relative membrane leakage (A) and malondialdehyde (MDA) (B) in leaves of *Arabidopsis thaliana* (*Col*, *CHS1*, *CHS2*, *CHS3*, *tt4*) exposed to 200 μmol m^{-2} s^{-1}. Data are mean ± SE (n = 4).

Table1 Primers used in RT-PCR assays

Gene ID	Primer name	Primer sequence (5'-3')
AT5G13930	*CHS*-F	TAGGTACCCATGGTGATGGCTGGTGCTTC
	CHS-R	TAGGATCCTTAGAGAGGAACGCTGTGCAAG

Table2 Summary of primers used in real-time qRT-PCR assays

Gene ID	Gene name	**Primer sequence**
AT5G62690	*TUB*	Forward: 5′- CCAGCTTTGGTGATTTGAAC -3′ Reverse: 5′- AAGCTTTCGGAGGTCAGAG -3′
AT5G13930	*CHS*	Forward: 5′- ACATCGTGGTGGTCGAAGTC -3′ Reverse: 5′- CCGGAGGTAGTGCAGAAGAC -3′
AT5G42800	*DFR*	Forward: 5′- ATGCCGCCTAGCCTTATCAC -3′ Reverse: 5′- AGCGTTGCATAAGTCGTCCA -3′
AT4G22880	*ANS*	Forward: 5′- AAGGCTCTCTCTGTCGGTCT -3′ Reverse: 5′- AACCCGGAACCATGTTGTGT -3′